Journal of Transportation System and Engineering, Vol.2
ISSN: 3059-9865(Print) 3059-9873(Online)
Volume 2, Issue 1 2026 (July):
DOI: https://doi.org/10.3126/jotse.v2i1.97155
Society of Transport Engineers Nepal (SOTEN)

Research Article
Received Date:02/10/2026
Accepted Date:05/14/2026
Published Date:07/14/2026

Landslide Susceptibility Mapping of the Beshisahar-Chame Mountain Road Segment, Nepal Using Geographic Information System and the Analytical Hierarchy Process

Deepak Timilsina[1], Buddhi Raj Joshi[1], Sundar Adhikari[1], Rajendra Aryal[1]*
[1] School of Engineering, Faculty of Science and Technology, Pokhara University, Nepal

Abstract

Landslides represent an incessant natural hazard in the mountainous topography of Nepal, where steep slopes, complex geology, intense monsoonal rainfall, and speedily expanding road infrastructure interact to magnify slope instability. This study evaluates anticipated landslide susceptibility along the Beshisahar-Chame mountainous road segment in central Nepal using a geographic information system (GIS) based multi-criteria decision analysis framework. Ten crucial landslide conditioning factors were considered, including slope, aspect, curvature, geology, soil type, land use and land cover, rainfall, drainage density, distance to drainage, and distance to road. The Analytical Hierarchy Process (AHP) was employed to derive relative weights for each factor through pairwise comparisons, confirming consistency of expert judgment. Separate thematic layers were generated from digital elevation models, satellite imagery, published datasets, and landslide inventory in the field, and successively integrated using weighted overlay analysis within a GIS surroundings. The resulting landslide susceptibility map categorises the study area into five zones which are very low, low, moderate, high, and very high susceptibility. Results point that 12.32% of the segment falls within very high susceptibility zones, while 29.23% and 33.55% are considered as high and moderate susceptibility, respectively. Highly susceptible areas are primarily associated with steep, south-facing slopes, weak and fractured lithologies, proximity to roads and drainage networks, and zones of extreme rainfall. The findings spotlight the dominant role of geology, slope gradient, and anthropogenic interventions, particularly unplanned road construction, in prompting landslides. The susceptibility map provides a powerful spatial structure for disaster risk reduction, infrastructure planning, and slope management, aiding informed decision-making for safer road development and sustainable land-use planning in the Himalaya territory.

Keywords: Landslide Susceptibility; GIS; AHP; Mountain Roads; Himalaya; Nepal

1. Introduction

Nepal is a predominantly mountainous country where landslides constitute one of the most recurrent and damaging natural hazards caused by its steep, rugged terrain. The term Landslide extends over a wide range of processes involving the downslope movement of slope-creating materials, including rock, soil, artificial fill, or their combinations. These materials may move through falling, toppling, sliding, spreading, or flowing mechanisms (Cruden and Varnes, 1996; Highland, 2004). The Nepalese mountains are geologically newly formed with high tectonic influence, resulting in steep slopes and inherently unstable landscapes. In a country where more than 80% of the land surface lies on slopes, landslides are not a new occurrence and many befall naturally. Besides topographic and geological conditions, unsuitable land-use practices, ongoing tectonic activity, and adverse climatic conditions considerably worsen landslide occurrence (Upreti and Dhital, 1996).

Intense and prolonged rainfall, particularly during the monsoon season, triggers extensive landslides, erosion, and slope failures across the country. Landslides are among the most destructive natural hazards in mountainous regions such as the Himalayas, initiating substantial economic losses and several fatalities every year. A major contributor to the increasing frequency of landslides is random rural road construction, often undertaken without adequate geotechnical attention, combined with rapid land-use and land-cover changes. Local geology and slope characteristics extra play a decisive role in controlling landslide initiation and distribution (Dhital, 1994).

To decrease losses associated with landslides, it is necessary to identify landslide-prone areas through systematic landslide susceptibility zonation. Landslide hazard or susceptibility zonation denotes to the delineation and mapping of areas with similar probabilities of landslide occurrence within a specified time period. Such maps

Corresponding Author's Email Address: raryalsr@gmail.com

are valuable tools for estimating, managing, and mitigating landslide hazards and for supporting land-use planning and infrastructure development (Ives and Messerli, 1981; Varnes, 1984). Landslides impose a worldwide serious threat to life and livelihoods, ranging from localized social disruption to comprehensive economic disasters. However, much of the existing work on landslide hazard assessment has been site-specific and predominantly driven by development projects and engineering requirements (Crozier and Glade, 2005).

2. Literature Review

Emerging attention to landslide studies in a global scenario reflects increasing awareness of their socio-economic impacts and the rising pressure of urbanization and infrastructure expansion in mountainous environments (Aleotti and Chowdhury, 1999). Landslides are normally defined as the movement of a mass of rock, debris, or earth downslope under the influence of gravity (Cruden, 1991). Various physical factors contribute directly or indirectly to landslide occurrence and are mainly categorized as intrinsic and extrinsic factors. Intrinsic factors contain geology, geomorphology, soil depth and type, slope gradient, slope aspect, elevation, land-use pattern, drainage characteristics, lineament density, and curvature, whereas extrinsic factors cover rainfall, earthquakes, and volcanic activity (Dai et al., 2001; Dahal et al., 2008). Extensive evaluation of these factors is essential for effective landslide hazard assessment and damage reduction (Anbalagan, 1992; Raghuvanshi et al., 2014a).

Current research and studies consistently reveal the effectiveness of GIS-based multi-criteria decision-making approaches for landslide susceptibility mapping along mountain road segments, delivering a robust scientific basis for the proposed study on the Beshisahar-Chame road corridor in Nepal. The Analytical Hierarchy Process has been widely applied to integrate geomorphological, geological, hydrological, and anthropogenic factors influencing slope instability (Achour et al., 2017; Banerjee et al., 2018; Jazouli et al., 2019; Panchal and Shrivastava, 2022). Susceptibility assessments focused to road indicates the critical role play of cut slopes, drainage modification, and traffic-induced disturbances in increasing landslide occurrence (Arsyad and Hamid, 2020; Sharma and Prakash, 2023).

In the Himalayan context, several studies confirm the suitability of AHP and hybrid methods for complex mountain topography designated by high relief, active tectonics, and intense monsoon rainfall (Kayastha et al., 2013; Singh and Kumar, 2018; Sur et al., 2020). Comparative analyses additionally indicate that AHP-based models produce reliable susceptibility zonation when validated against landslide inventories, particularly in regions with limited data (Bhatt et al., 2013; Noorollahi et al., 2018; Gautam et al., 2021). Contemporary improvements in research incorporate machine learning to enrich prediction accuracy; however, AHP remains in favour for transparent weighting and practical applicability in infrastructure planning (Dou et al., 2023; Sun et al., 2023). Moreover, integrating susceptibility outcomes with road vulnerability helps risk-informed land-use and transportation management (Roccati et al., 2021; Yousefi et al., 2022; Zhou et al., 2024).

Also, the recent AHP study by Subedi et al. (2023) in Gandaki province confirmed the efficacy of the method (AUC=0.793) and identified major factors such as slope (25.5% weight) and proximity to roads. This aids an important basis and validates the application of AHP for a comprehensive, infrastructure-centric assessment along the Beshisahar-Chame road segment. As a whole, these studies substantiate the methodological framework and regional relevance of basis for GIS-AHP applied landslide susceptibility mapping for mountainous roads in Nepal.

This research aims to cooperate with government agencies and policymakers by providing scientific efforts for effective surveying, planning, and construction of transportation routes on stable slopes, along with informed implementation of development activities. The study concentrates on the preparation of a landslide susceptibility map and the classification of areas into very low, low, moderate, high, and very high susceptibility zones. The expected outcomes are assumed beneficial to local communities, researchers, and stakeholders involved in disaster risk reduction and management. Although a few studies have addressed landslide susceptibility within Lamjung District, a widespread assessment along the entire 66.2 km Beshisahar-Chame road segment has not yet been conducted. This research therefore pursues to evaluate the overall feasibility of the Beshisahar-Chame road, identify the most vulnerable sections of the landscape, and offer a scientific base for targeted landslide mitigation measures along the route.

3. Methodology:

3.1 Study Area

The study was steered along the Marsyangdi River basin, extending from Khudi in Lamjung District to Chame in Manang District, central Nepal. Referring Figure 1a, the study area situates between latitudes 28.25° N to 28.52° N and longitudes 84.33° E to 84.24° E. The southern part of the study segment falls within Lamjung District, while the northern section resides in Manang District. The area also includes a segment of the famous Annapurna Base Camp trekking route. The terrain is considered by rugged and steep topography, as reflected by an evident altitudinal variation ranging from approximately 820 m at Bhulbhule to about 2650 m at Chame.

Figure 1a: Map of Nepal with Proposed Road Segment (Source: Google Maps)

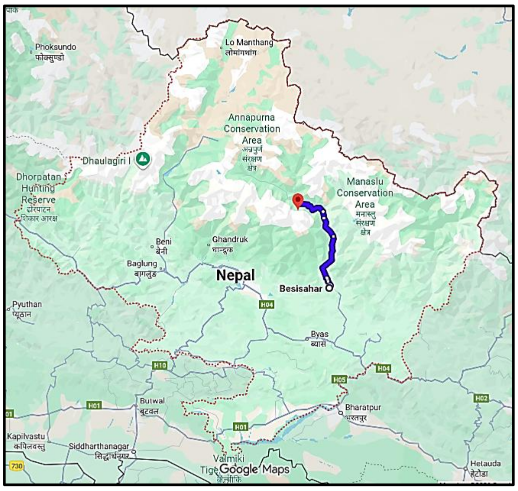

Figure 1b: Map of Gandaki Province with Proposed Road (Source: Google Maps)

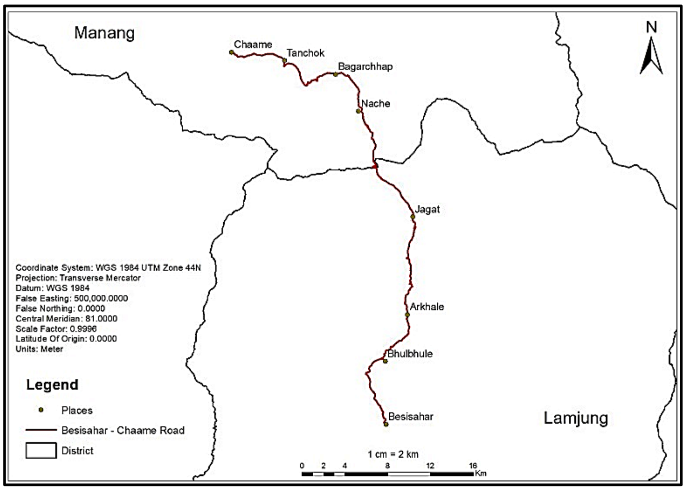

Figure 1c: Location Map of the Road Segment

3.2 Workflow of the Study

Landslide hazard susceptibility maps can be generated using different approaches, including heuristic, statistical, and deterministic models. In this study, a heuristic approach was adopted to prepare the landslide susceptibility map. This approach is based on expert knowledge and experience, in which causative parameters to landslide event are identified, weighted, and relative ratings are allocated. These weighted parameters are then integrated to generate a landslide susceptibility map.

The heuristic model obeys a hierarchical association of conditioning factors and allows experts to assign weights to each factor based on its relative influence on landslide occurrence. The fundamental concept consists of assigning weights to thematic layers representing vital variables controlling landslides. A combination rule is subsequently applied to integrate all weighted layers and produce a composite susceptibility index. The resultant index map is then classified into susceptibility classes, and areas prone to landslides are delineated accordingly (Abella and van Westen, 2001).

3.3 Steps of the Study

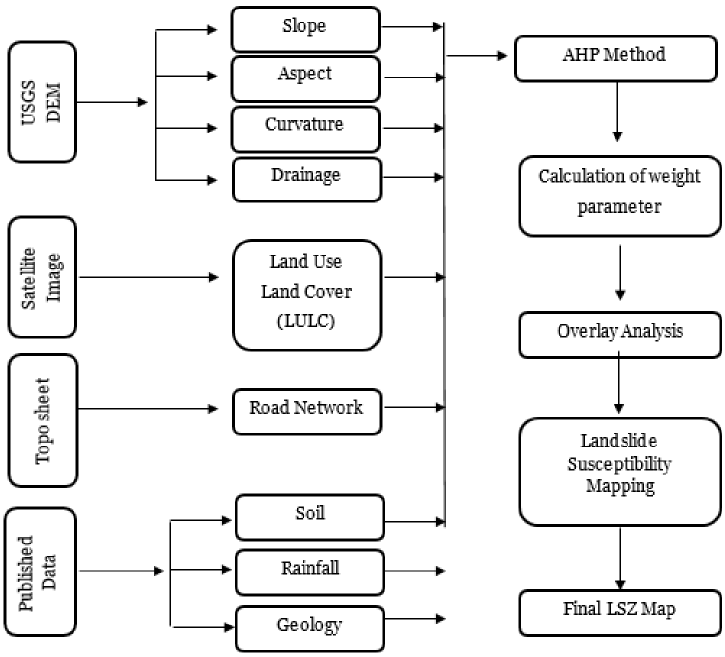

Figure 2: Conceptual Framework of the Study

Figure 2 presents the conceptual framework of the study, which follows a standard methodological approach largely used in landslide susceptibility mapping through GIS integrated with the AHP. The methodology includes several sequential steps. First, a comprehensive landslide inventory map is prepared, serving as the primary dataset for analysis. Second, relevant physical factors influencing slope instability, either directly or indirectly, are identified, and thematic maps for each factor are generated. Third, these factors are scientifically evaluated using AHP to determine their relative importance in landslide occurrence. Finally, the weighted thematic layers are integrated within a GIS settings to produce a detailed landslide susceptibility map. This map provides a systematic basis for landslide hazard assessment, risk evaluation, and spatial planning in the study area.

3.4 Data and Software

This research uses a combination of primary and secondary data sources, analysed through dedicated geospatial software. A Digital Elevation Model (DEM) with a spatial resolution of 30 m (SRTM) was employed for terrain analysis. This resolution is broadly recognized for regional to corridor-scale landslide susceptibility studies, as it offers an satisfactory balance between computational efficiency and representation of terrain variability along linear infrastructure such as mountain roads. Primary data was collected directly from the field by means of photographs and interviews with local residents. Secondary data comprised of published literature and, remarkably, several spatial datasets like a Digital Elevation Model (DEM), topographic maps, Open Street Map (OSM) data, and satellite imagery from Google Earth Pro etc. The major analytical work was accomplished using ArcGIS, the key platform for managing, analysing, and mapping all data to prepare hazard assessments. Google Earth Pro accompanied this by providing detailed 3D visualization and base imagery for the study area.

4. Results and Discussion

4.1 Causative Factors of Landslides

A landslide event happens when the resisting strength of soil or rock forming a slope is exceeded by gravitational forces. This equilibrium may be put on upset by both natural and anthropogenic processes. Slope instability and landslide occurrence are controlled by several interacting factors that often operate in complex and subtle ways (Varnes, 1978). The selection of causative factors is thus reliant on the dominant types of landslide and the geo-environmental features of the study area (Ayalew et al., 2005).

Customary causative factors include elevation, slope gradient, slope aspect, rainfall, curvature, proximity to drainage networks, proximity to roads, and land use-land cover. These factors can be broadly characterised into geological, morphological, and anthropogenic controls. Geological factors comprise the presence of soft or highly fractured rocks such as phyllites, slates, and schists; calcareous interlayers that endorse dissolution, formation of void, and high porosity; intense weathering; sheared, jointed, or fissured materials; and rocks weakened by folding and faulting with unfavourably oriented discontinuities. Morphological factors contain tectonic and seismic activity, fluvial erosion at slope toes, undercutting of riverbanks by deeply cut streams, high relief and steep slopes, slope shape, and slope aspect. The Himalayan region is situated within a zone of high seismicity, further promoting slope instability. Concentrated precipitation is one of the most protruding triggering factors in the study area, where a large proportion of annual rainfall event occurs within less than three months during the monsoon season.

Anthropogenic factors play an increasingly vital role in landslide initiation. These include deforestation on hill slopes, improper land-use practices such as cultivation and irrigation on steep landscape, overgrazing, quarrying for construction materials without regard to topographical stability, and insufficient evaluation of slope conditions in focused to infrastructure development in hilly areas.

4.2 Thematic Maps Used in the Study

Ten landslide conditioning factors were considered in the analysis which are slope, aspect, geology, rainfall, land use and land cover, soil type, drainage density, distance to drainage, distance to road, and curvature. Besides, an elevation map representing terrain variation and a landslide inventory map showing the spatial distribution of existing landslides were prepared for the study area. These thematic layers formed the foundation for landslide susceptibility analysis.

4.2.1 Elevation Map

The elevation map denotes the spatial distribution of altitude within the study area, referenced to mean sea level and measured in metres. As presented in Figure 3a, elevation was classified into six categories, each represented by a distinct colour. The map illustrates considerable altitudinal variation across the study segment, reflecting the rough Himalayan terrain.

4.2.2 Landslide Inventory Map

A total of 5 landslides were observed within and near the Beshisahar-Chame road corridor as shown in Figure 3b. These contain debris flows, shallow slides, and rockfalls. The inventory was prepared employing a combination of field surveys, clarification of high-resolution satellite imagery, and secondary reports. Approximately 70% of the mapped landslides were used for model calibration, whereas the lasting 30% were kept for independent validation.

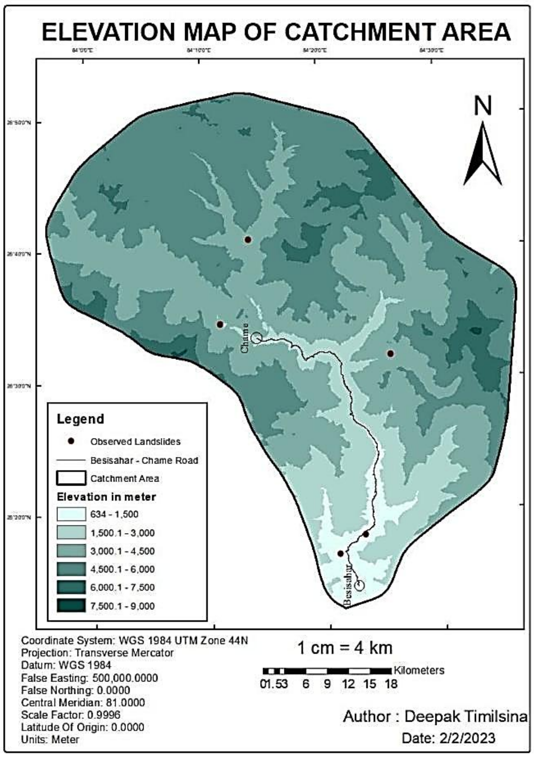

Figure 3a: Elevation Map of Study Area

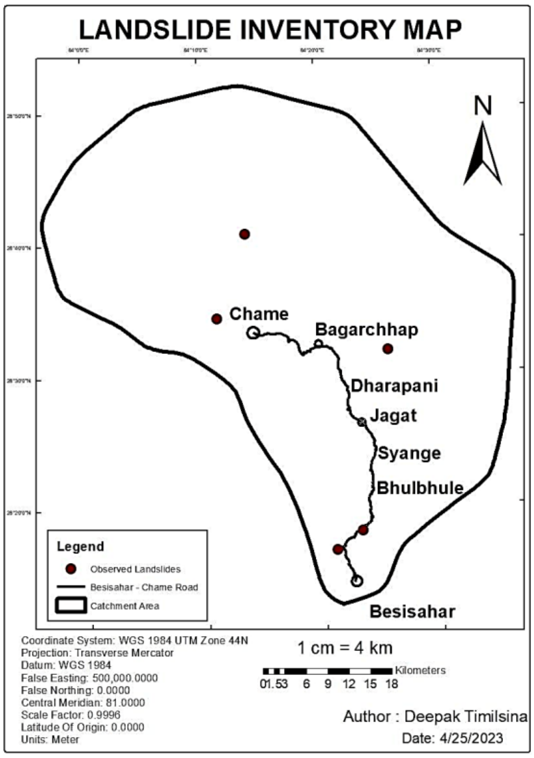

Figure 3b: Landslide Inventory Map of Beshisahar-Chame Road Segment

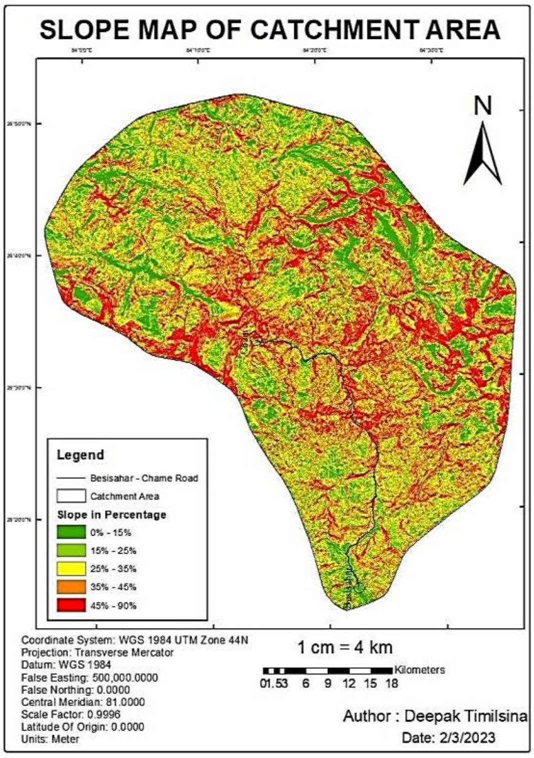

Figure 3c: Slope Map from DEM

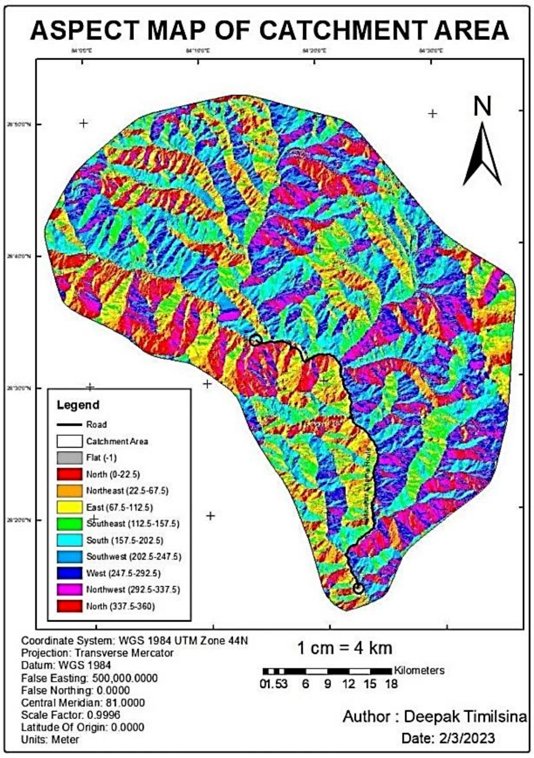

Figure 3d: Aspect Map of Study Area

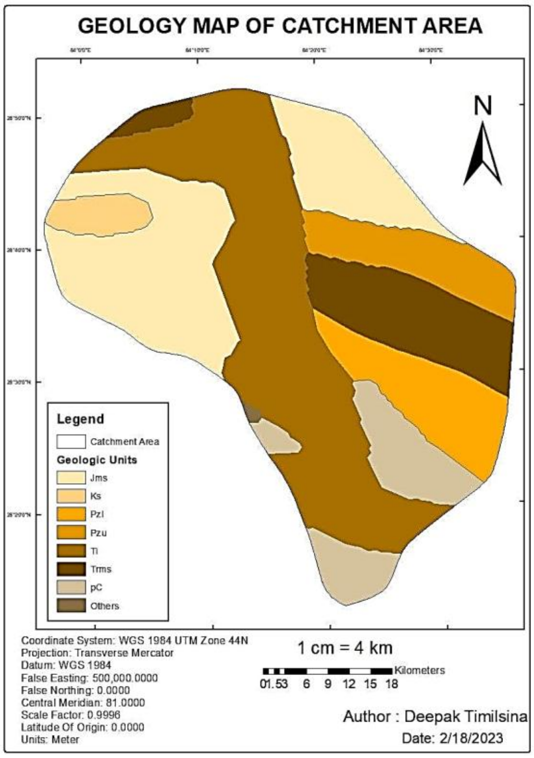

Figure 4a: Geological Map of the Study Area

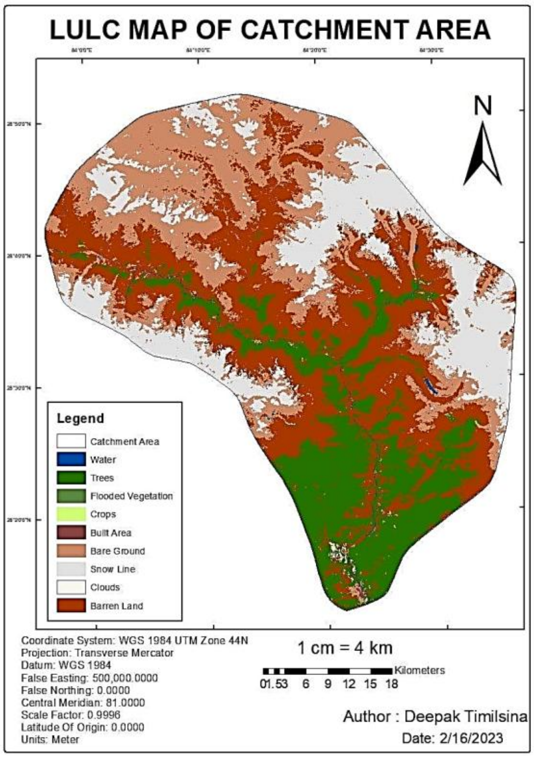

Figure 4b: LULC Map of the Study Area

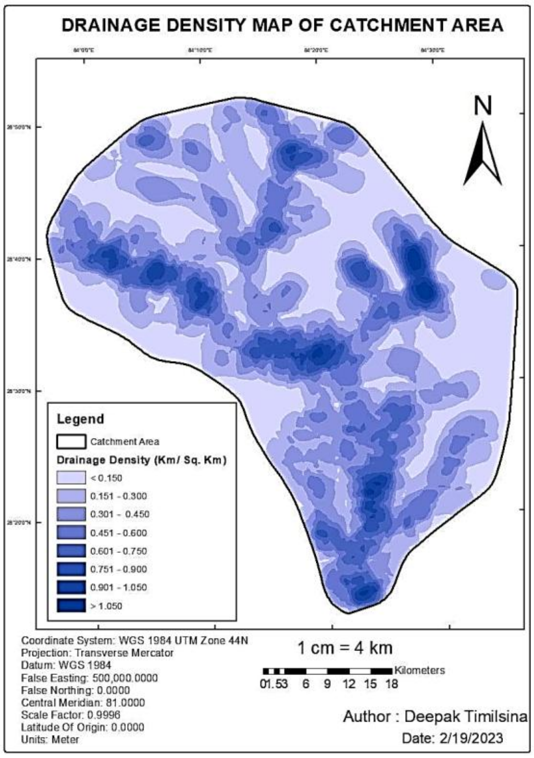

Figure 4c: Map Showing Drainage Density

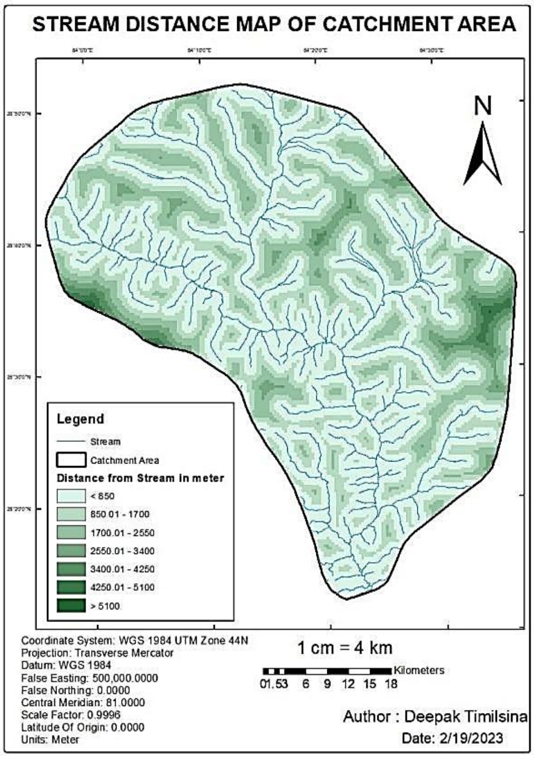

Figure 4d: Map Showing Distance to Drainage

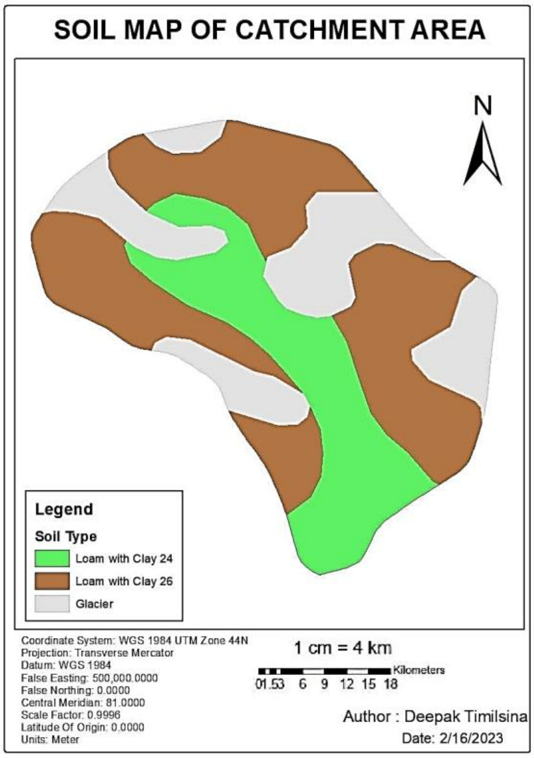

Figure 5a: Map Showing Soil Type of the Study Area

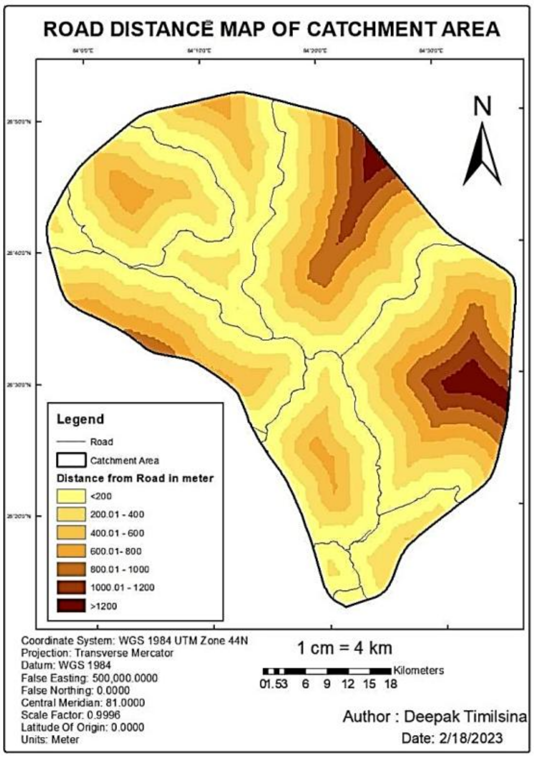

Figure 5b: Map Showing the Distance to Road

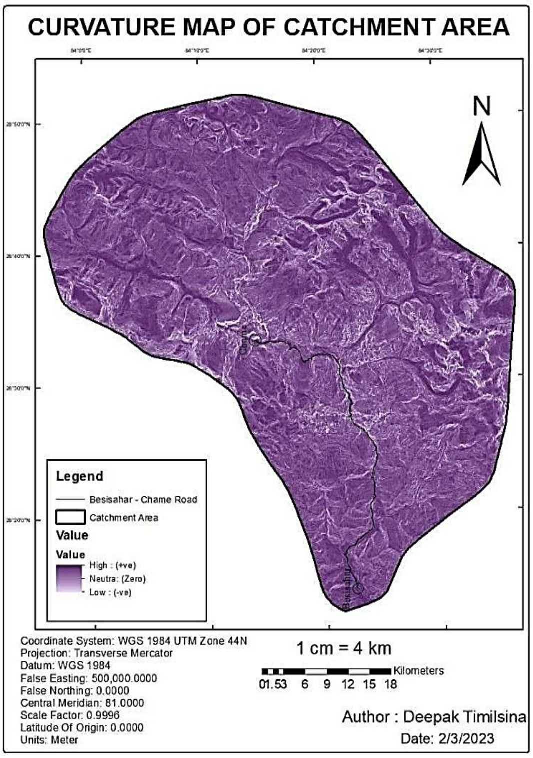

Figure 5c: Map Showing the Curvature in the Study Area

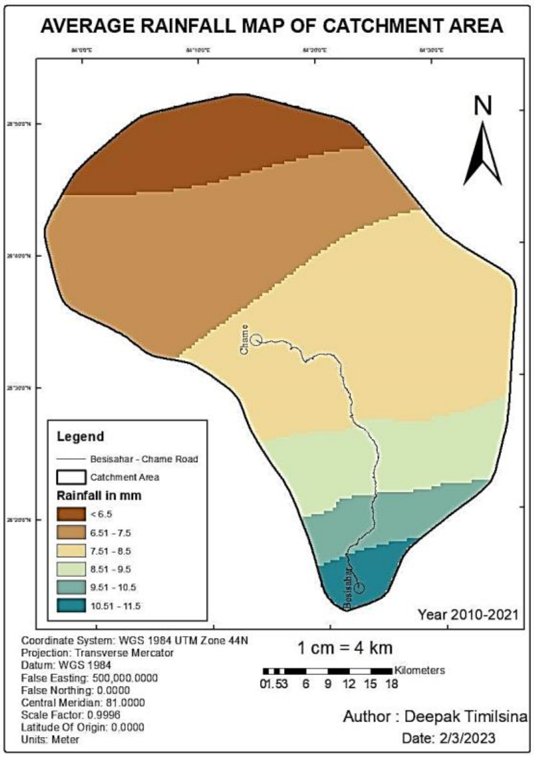

Figure 5d: Map Showing the Rainfall in the Study Area

4.2.3 Slope Map

The slope map of the Beshisahar-Chame road section is presented in Figure 3c. Slope angles were derived from the digital elevation model (DEM) and classified into five categories as 0-15°, 15-25°, 25-35°, 35-45°, and 45-90°. Each class is denoted by a distinct colour, spot lighting the predominance of steep slopes along the segment.

4.2.4 Aspect Map

Figure 3d demonstrates the aspect map of the study area, classified into nine directional categories as North (0°), Northeast, East (90°), Southeast, South (180°), Southwest, West (270°), Northwest, and flat surfaces. Flat areas were given an aspect value of minus 1. Aspect influences microclimatic conditions, soil moisture, and vegetation cover, thus affecting landslide susceptibility.

4.2.5 Geology Map

The geological map in Figure 4a indicates that the study area includes Jurassic metamorphic and sedimentary rocks (Jms), Cretaceous sedimentary rocks (Ks), Lower Paleozoic rocks (Pzl), Upper Paleozoic rocks (Pzu), Tertiary igneous rocks (Ti), Triassic metamorphic and sedimentary rocks (Trms), and undivided Precambrian rocks (Pc). Areas classified as "no data" relate to locations where geological information was unobtainable.

4.2.6 Land Use and Land Cover Map

The land use and land cover (LULC) map presented in Figure 4b recognises water bodies, tree cover, grassland, flooded vegetation, cropland, shrub or scrub areas, built-up areas, bare ground, and snow cover. LULC plays a decisive role in slope stability by prompting surface runoff, infiltration, and root reinforcement.

4.2.7 Drainage Density Map

Figure 4c shows the drainage density map, classified into five categories as 0-0.150, 0.150-0.300, 0.300-0.450, 0.450-0.600, and >0.600 km/km². Higher drainage density reflects increased surface dissection and potential slope instability.

4.2.8 Distance to Drainage Map

The distance to drainage map in Figure 4d was considered into six classes: 0-850 m, 850-1700 m, 1700-2550 m, 2550-3400 m, 3400-4250 m, and >4250 m. Proximity to drainage networks stimulates erosion, toe undercutting, and pore-water pressure conditions.

4.2.9 Soil Type Map

As presented in Figure 5a, the study area is largely classified into three soil categories: loam with clay (Zu), loam with clay (Zl), and glacier deposits. Soil type affects shear strength, permeability, and weathering performance which influences landslide event to occur.

4.2.10 Distance to Road Map

Figure 5b clarifies the distance to road map, classified into six distance categories matching to those used for distance to drainage. Roads habitually act as destabilizing elements because of slope cutting, inadequate drainage, and vibration loads.

4.2.11 Curvature Map

The curvature map in Figure 5c was classified into three types such as positive (convex), zero (flat), and negative (concave). In the Beshisahar-Chame segment, 63.44% of the area exhibits positive curvature, 6.98% negative curvature, and 29.57% flat terrain. Convex slopes are generally more likely to landslides as a result of tensile stress development and reduced material support. Consequently, higher weight was assigned to positive curvature and moderate weight to negative curvature, following previous studies (Ahmed, 2015; Ayalew et al., 2005; Roslee et al., 2017).

4.2.12 Average Rainfall Map

The rainfall map signifies average annual precipitation (mm/year) derived from Department of Hydrology and Meteorology (DHM), Nepal, covering the period 2000–2020. Rainfall was categorised into six value ranges: <1500, 1500–2000, 2000–2500, 2500–3000, 3000–3500, and >3500 mm/year as shown in Figure 5d. Landslide Susceptibility Mapping Using AHP

4.3 Analytical Hierarchy Process Method

The AHP is a semi-quantitative method in which decisions are taken using weights through pair-wise relative comparisons without inconsistencies in the decision process (Saaty, 1990). The pairwise comparisons and weight assignments were accomplished based on a combination of expert judgment and literature review. A panel of three experts in geotechnical engineering and geomorphology contributed to the weighting process, aided by past published studies in Himalayan terrain. The AHP consists of following five steps: (i) break down a decision problem into component factors; (ii) arrangement of these factors in a hierarchic order; (iii) assignment of numerical values to determine the relative importance of each factor according to their subjective relevance; (iv) set up of a comparison matrix; and (v) computation of the normalized principal eigenvector, which gives the weight of each factor. The pairwise comparison matrix grows quadratic, with respect to the number of parameters and subclasses. This method helps to capture subjective aspects of the decision (Saaty, 1990).

4.3.1 Construction of Pair-wise Comparison Matrix

The pair wise comparison matrix for the ten parameters and the subclasses are obtained by rating each parameter against every other parameter by assigning a relatively dominant value between 1 and 9 to the intersecting cell as given in Table 1. The real relationship was rated as whole number and its reversal relationship was rated as its fractional value. A quadrilateral matrix was framed as given in equation 1 and given in Table 1.

$$A = \begin{bmatrix} 1 & a_{12} \ldots\ldots & a_{1n} \\ 1/a_{12} & 1 & a_{2n} \\ 1/a_{1n} & 1/a_{2n} & 1 \end{bmatrix} \ldots\ldots \text{Eq. (1)}$$

Table 1: Scale of Preference Used in AHP (Thomas L.Saaty, 1977, 2000)

Scale	Degree of Performance
1	Equal importance
3	Moderate importance of one factor over the other
5	Strong or essential importance
7	Very strong importance
9	Extreme importance
2,4,6,8	Values for inverse comparison

In the matrix given in Annexure-I, when the column element dominates the row, the whole number was assigned, if the row element predominates, the inverse of the whole number was assigned. In this study, we can compare a pair-wise matrix was constructed from literature for all other parameters and factors with diagonal values equal to 1. In the pair-wise comparison matrix, the upper and lower half of the diagonal was symmetrical and hence their values of them were reciprocal to each other. The geometric mean was calculated for each row of the matrix and the same was divided by the total geometric mean of the column to determine the weights of the row element. The weights thus determined were normalized so that their summation equals one and is known as priority eigenvector as explained in the Annexure-I. The same procedure was followed for each class and their respective subclass and checked for consistency.

4.3.2 Evaluation of the Comparison Matrix

In AHP, the consistency was checked by calculating the consistency ratio (C.R.) value using the equation 2. To determine Consistency Index (C.I.) value, Consistency Measure (C.M.) was calculated using matrix multiplication function MMULT () for the average value of weights as given in the Tables. From CM value, the maximum positive value (λ_{max}) was determined using Ms Excel. C.I. value is determined using the equation 2.

$C.R. = \frac{CI}{RI}$ ….. Eq. (2)

$C.I. = (\lambda_{max} - N)/(N - 1)$ ….. Eq. (3)

λ_{max} = largest positive eigen value

N – Order of matrix

Random Indices (R.I) value was selected from Table 2 for all 10 parameters. From CI and RI value CR was determined. The CR values equals to 0.093 less than 0.1 and hence the weight of the spatial parameters assigned were consistent and can be adopted. CR values close to 0 indicates the high probability (Saaty T. L., 1990). If CR value > 0.1 then the correlation matrix should be revised (Senouci et.al, 2021).

Table 2: Random Indices (Thomas L.Saaty, 2000)

N	1	2	3	4	5	6	7	8	9	10	11	12	13	14	15
R.I.	0	0	0.52	0.89	1.12	1.25	1.35	1.40	1.45	1.49	1.52	1.54	1.56	1.58	1.59

According to Saaty, the coherence ratio must be less than or equal to 10% or an imprecision of less than 10%. The principle consists in comparing the judgment with the random weighting of the elements. Finally, the acquisitive weights were integrated the various causative class in single landslide susceptibility index using this equation (Thomas L.Saaty, 2000)

$L.S.I. = \sum_{i=1}^{n} R_i * W_i$ …… Eqs.4

Where, R_i the rating is class, each layer and W_i is the weights for the each of the landslide conditioning factors. The resulting landslide susceptibility index (L.S.I.) map as classified into three classes (low, moderate and high) based on the natural breaks (Jenks) to define the class intervals in the landslide susceptibility map (Senouci et.al, 2021).

4.4 Generation of Landslide Susceptibility Map

The landslide susceptible map for the Beshisahar to Chame Section in Figure 6a is classified into five landslide susceptible regions i.e., very low, low, moderate, high and very high. From the above, the landslide is dominated by the geology of the study area. The areas having weak and highly fractured rocks are highly unstable as compared to the area having unfractured rocks. The study area can be now classified in five zones very highly susceptible zone (12.32%), highly susceptible zone (29.23 %), moderately susceptible zone (33.55%) and low susceptible zone (20.60%) and very low susceptible zones (4.25%) . High susceptibility zones are strongly related with Jurassic metamorphic rocks (Jms) and Triassic formations (Trms), which shows high fracturing and weathering natures.

Table 3: Area Distribution under Susceptibility Class

SN	Hazard	Area(sq.km)	Percentage
1	Very Low	11.453	4.25
2	Low	55.30	20.60
3	Medium	90.10	33.55
4	High	78.47	29.23
5	Very High	33.9	12.32
Total			100.00

The data is summarized in Table 3. The majority of landslide can be seen on the road and river corridor in the study area. The south facing and highly steep slopes are highly susceptible in the northern portion. Here, major contributing component is slope, aspect and LULC etc.

4.5 Validation and Transferability in Global Context

The receiver operating characteristic (ROC) validation was completed using the 30% held-out landslide dataset that was not utilised during model calibration, confirming independent assessment of predictive performance. The area under the curve (AUC) value of 0.733 as shown in Figure 6b, calculated by means of the Arc SDM extension in ArcMap 10.8, shows a trustworthy model performance, as values above 0.5 denote correctness while those below suggest randomness. This result exhibits satisfactory agreement between the predicted susceptibility map and observed landslide locations, approving the model’s efficiency for landslide susceptibility mapping.

The validation ratifies the consistency of the model and recommends potential for global transferability by the AUC value of 0.733 which considerably surpasses the random threshold of 0.5. The attained AUC value of 0.733 is comparable to similar Himalayan corridor studies, where AUC values normally range between 0.70 and 0.85 (e.g., Kayastha et al., 2013; Subedi et al., 2023). This implies satisfactory predictive capability for regional planning and engineering applications. This performance attained using commonly accessible ROC curve methodology and ArcGIS software, shows that the applied analytical framework is strong. Such a standardized validation approach boosts the model's suitability for application in other areas with similar geo-environmental situations, backing up its larger utility in landslide susceptibility assessments in world community.

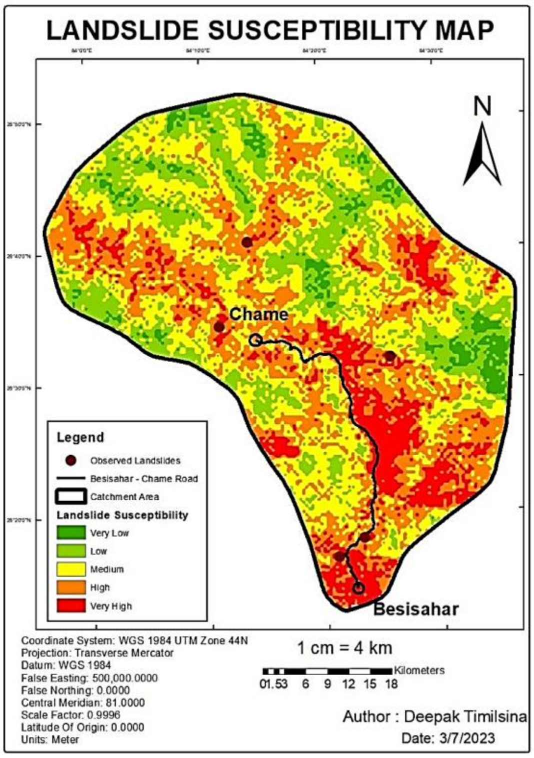

Figure 6a: Landslide Susceptibility Mapping of Beshisahar-Chame Road Segment

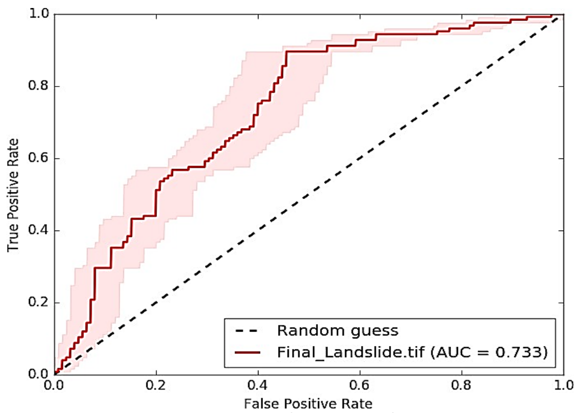

Figure 6b: Assessment of Model Performance Based on the ROC Curve

As compared to adjacent Himalayan corridor studies, the current findings align with observed dominance of slope and geology as main controlling factors, although marginally lower AUC advises scope for integration of machine learning methods.

5. Conclusion

This study offers a GIS-based landslide susceptibility assessment for the Beshisahar-Chame mountainous road corridor using a heuristic Analytical Hierarchy Process integrated with multi-source spatial data. Ten causative factors on behalf of geo-morphological, geological, hydrological, climatic, land-use, and anthropogenic controls were methodically weighted and combined to delineate landslide susceptibility zones. The consistency ratio obtained for the AHP matrix confirmed the sturdiness and internal coherence of the weighting scheme, aiding the reliability of the last susceptibility outcomes.

The results signify that nearly 3/4th of the study area falls within moderate to very high susceptibility classes, with high and very high hazard zones jointly covering more than 40% of the segment. These zones are primarily concentrated along steep south-facing slopes, river valleys, and road-aligned cut slopes, emphasizing the combined influence of slope gradient, aspect, weak and fractured lithology, proximity to drainage networks, and haphazard road construction. Rainfall appears as a critical triggering factor during the monsoon season by elevating pore water pressure and falling shear strength, while fluvial undercutting and poor drainage management additionally worsen slope instability. Anthropogenic interventions particularly ineffectively engineered road alignments, slope excavation without stabilization procedures, and insufficient surface and subsurface drainage pointedly intensify landslide susceptibility even in areas that are otherwise moderately stable.

The generated landslide susceptibility map provides a spatially clear and decision-oriented framework for hazard mitigation along a strategically important Himalayan road segment. It presents direct utility for land-use planning, infrastructure design, slope management, and disaster risk reduction by enabling prioritization of segments on high-risk for detailed geotechnical investigation and targeted stabilization way-out. The findings essentially stress that even low-susceptibility zones can rapidly undergo transition to higher risk categories under haphazard development practices featuring the need for proactive planning and strict obedience to engineering and environmental precautions.

Slope stabilization techniques like retaining structures and bioengineering methods are highly recommended near Bhulbhule-Ngadi section, where as realignment or controlled excavation strategies should be prioritized in steep sections near Tal-Chame segment.

Finally, the outputs of the assessment prove that GIS and AHP based susceptibility mapping is an effective and transferable approach for mountainous topography of Nepal. The findings contribute to a clearer approval of landslide controls in the Marsyangdi River basin and provide practical guidance for planners, engineers, and disaster management authorities to reduce forthcoming landslide impacts on lives, infrastructure, and livelihoods along the Beshisahar-Chame road segment. However, the study is focused to limitations containing subjectivity in AHP weight assignment, resolution limits of DEM data, and inadequate temporal landslide inventory.

Supplementary Materials: No supplementary material is required and available in this study.

Author Contributions: Data collection, data preparation, data management, methodology development, landslide susceptibility mapping and analysis, and manuscript draft preparation were all accomplished by D.T., B.R.J. contributed on model analysis, data verification, and draft enhancement. S.A. contributed for additional conceptualization, draft paper revision with feedback correction. R.A. supervised with inclusive insight, modification, addition and finalization of the manuscript. All authors have read and agreed to the published version of the manuscript.

Informed Consent Statement: Informed consent was obtained from all subjects involved in the study.

Data Availability Statement: This research used various data such as the primary data (photographs, interviews) assisting this research and secondary geospatial data (DEM, maps) are from public repositories or reliable sources along with derived susceptibility maps and processed datasets will be provided upon a written request to the corresponding author by email.

Acknowledgements: The authors appreciatively acknowledge the use of publicly offered geospatial datasets, containing DEM, geological maps, rainfall data, and satellite imagery attained from national and international sources. ArcGIS software and Google Maps were employed for data processing, spatial analysis, and visualization indispensable to the effective completion of this research. The authors highly acknowledge Associate Prof. Dr. Rajib Pokhrel for invaluable support and feedbacks. The authors would also like to acknowledge all the supporting hands for this research. Furthermore, the authors gratefully acknowledge *Society of Transport Engineers-Nepal* for creating platform to publish the research paper under *Transportation Engineering and Infrastructures*.

Conflicts of Interest: The authors declare no personal or institutional conflicts of interest.

References

Abella, EC., Van, Westen CJ. (2001) Landslide hazard assessment using the heuristic model. In: Proceedings of the IV Congreso de Geología y Minería, Ecuador

Achour, Y., Boumezbeur, A., Hadji, R., Chouabbi, A., Cavaleiro, V., Bendaoud, EA. (2017) Landslide susceptibility mapping using analytic hierarchy process and information value methods along a highway road section in Constantine, Algeria. Arab J Geosci 10(8):194. https://doi.org/10.1007/s12517-017-2980-6

Ahmed, B. Landslide susceptibility mapping using multi-criteria evaluation techniques in Chittagong Metropolitan Area, Bangladesh. *Landslides* 12, 1077–1095 (2015). https://doi.org/10.1007/s10346-014-0521-x

Aleotti, P., & Chowdhury, R. (1999). Landslide hazard assessment: Summary review and new perspectives. *Bulletin of Engineering Geology and the Environment*, 58(1), 21–44. https://doi.org/10.1007/s100640050066

Anbalagan, R. (1992). *Landslide hazard evaluation and zonation mapping in mountainous terrain*. *Engineering Geology, 32*(4), 269–277. https://doi.org/10.1016/0013-7952 (92)90053-2

Arsyad, A., Hamid, W. (2020) Landslide susceptibility mapping along road segments in west Sulawesi using GIS-AHP models. https://iopscience.iop.org/article/10.1088/1755-1315/419/1/012080

Ayalew, L., Yamagishi, H., Marui, H., Kanno, T. (2005) Landslides in Sado Island of Japan. Part II: GIS-based susceptibility mapping. Eng Geol 81(4):432–445. https://doi.org/10.1016/j.enggeo.2005.08.004

Banerjee, P., Ghose, MK., Pradhan, R. (2018) Analytic hierarchy process and information value method-based landslide susceptibility mapping and vehicle vulnerability assessment along a highway in Sikkim Himalaya. Arab J Geosci 11(7):139. https://doi.org/10.1007/s12517-018-3488-4

Bhatt, BP., Awasthi, KD., Heyojoo, BP., Silwal, T., Kafle, G. (2013) Using geographic information system and analytical hierarchy process in landslide hazard zonation. Appl Ecol Environ Sci 1(2):14–22. Doi: 10.12691/aees-1-2-1

Glade, T., Anderson, M., & Crozier, MJ. (Eds.). (2005). *Landslide hazard and risk*. John Wiley & Sons. https://doi.org/10.1002/9780470012659

Cruden, DM. (1991). *A simple definition of a landslide*. *Bulletin of the International Association of Engineering Geology*, *43*(1), 27–29. https://doi.org/10.1007/BF02590167

Cruden, DM., Varnes, DJ. (1996) Landslide types and processes. In: Turner AK, Schuster RL (eds) Landslides: investigation and mitigation. Transportation Research Board Special Report 247, National Research Council, Washington, DC, pp 36–75

Dai, FC., Lee, CF., & Ngai, YY. (2002). *Landslide risk assessment and management: An overview*. *Engineering Geology, 64*(1), 65–87. https://doi.org/10.1016/S0013-7952(01)00093-X

Dahal, RK., Hasegawa, S., Nonomura, A., Yamanaka, M., & Dhakal, S. (2008). Predictive modelling of rainfall-induced landslide hazard in the Lesser Himalaya of Nepal based on weights-of-evidence. *Geomorphology, 102*(3-4), Article 0169-555X. https://doi.org/10.1016/j.geomorph.2008.05.041

Dhital, MR. (1994) Damage due to catastrophic floods and landslides in the Sun Koshi area and the need for hazard assessment in the Himalaya. ICIMOD, Kathmandu

Dou, H., Huang, S., Jian, W., Wang, H. (2023) Landslide susceptibility mapping of mountain roads based on machine learning combined model. J Mt Sci 20(5):1232–1248. https://doi.org/10.1007/s11629-022-7657-2

Gautam, P., Kubota, T., Sapkota, LM., Shinohara, Y. (2021) Landslide susceptibility mapping with GIS in high mountain area of Nepal: A comparison of four methods. Environ Earth Sci 80(9):359. https://doi.org/10.1007/s12665-021-09650-2

Ives, JD., Messerli, B. (1981) Mountain hazards mapping in Nepal. Mt Res Dev 1(3/4):223–230. https://doi.org/10.2307/3673059

Jazouli, AE., Barakat, A., Khellouk, R. (2019) GIS-based multi-criteria evaluation using AHP for landslide susceptibility mapping. Geoenviron Disasters 6:3. https://doi.org/10.1186/s40677-019-0119-7

Kayastha, P., Dhital, MR., & De Smedt, F. (2013). Application of the analytical hierarchy process (AHP) for landslide susceptibility mapping: A case study from the Tinau watershed, west Nepal. *Computers & Geosciences, 52*, 398–408. https://doi.org/10.1016/j.cageo.2012.11.003

Ministry of Home Affairs (2019) Disaster risk reduction status report. Government of Nepal, Kathmandu

Noorollahi, Y., Sadeghi, S., Yousefi, H., Nohegar, A. (2018) Landslide susceptibility mapping using AHP and fuzzy logic. Int J Hydrol 2(2):142–153. DOI 10.15406/ijh.2018.02.00063

Panchal, S., & Shrivastava, AK. (2022). *Landslide hazard assessment using analytic hierarchy process (AHP): A case study of National Highway 5 in India*. Ain Shams Engineering Journal, 13(3), 101626. https://doi.org/10.1016/j.asej.2021.10.021

Pokhrel, P., & Pathak, D. (2016). *Landslide susceptibility mapping of southern part of Marsyangdi River basin, West Nepal using logistic regression method*. International Journal of Geomatics and Geosciences, 7(1), 24–32.

Raghuvanshi, TK., Ibrahim, J., & Ayalew, D. (2014). Slope stability susceptibility evaluation parameter (SSEP) rating scheme–an approach for landslide hazard zonation. *Journal of African Earth Sciences, 99*, 595–612. https://doi.org/10.1016/j.jafrearsci.2014.05.004

Roccati, A., Paliaga, G., Luino, F., Faccini, F., Turconi, L. (2021) GIS-based landslide susceptibility mapping for land use planning and risk assessment. Land 10(2):162. https://doi.org/10.3390/land10020162

Roslee, R., Mickey, AC., Simon, N., Norhisham, MN. (2017) *Landslide Susceptibility Analysis (LSA) Using Weighted Overlay Method (WOM) along the Genting Sempah to Bentong Highway, Pahang*. Malaysian Journal of Geosciences, 1(2):13–19. DOI: 10.26480/mjg.02.2017.13.19.

Saaty, TL. (1990). *How to make a decision: The analytic hierarchy process. European Journal of Operational Research, 48*(1), 9–26. https://doi.org/10.1016/0377-2217(90)90057-I

Saaty, TL. (1977). *A scaling method for priorities in hierarchical structures*. Journal of Mathematical Psychology, 15(3), 234–281. https://doi.org/10.1016/0022-2496(77)90033-5

Saaty, TL. (2000). *Fundamentals of decision making and priority theory with the analytic hierarchy process* (Vol. 6). RWS Publications.

Senouci, R., Taibi, NE., Teodoro, AC., Duarte, L., Mansour, H., & Yahia Meddah, R. (2021). *GIS-based expert knowledge for landslide susceptibility mapping (LSM): Case of Mostaganem Coast District, West of Algeria*. Sustainability, 13(2), 630. https://doi.org/10.3390/su13020630

Sharma, A., Prakash, C. (2023) Impact Assessment of Road Construction on Landslide Susceptibility in Mountainous Region using GIS-Based Statistical Modelling. J Geol Soc India 99(8):1131–1140. https://doi.org/10.1007/s12594-023-2439-1

Singh, K., Kumar, V. (2018) Hazard assessment of landslide disaster using information value method and analytical hierarchy process in highly tectonic Chamba region in bosom of Himalaya. J Mt Sci 15(4):808–824. https://doi.org/10.1007/s11629-017-4634-2

Subedi, S., Bhandari, KP., Sherchan, B., & Neupane, N. (2023). Landslide Susceptibility Mapping Using Analytical Hierarchy Process in Gandaki Province, Nepal. *Journal of Engineering and Sciences*, *2*(1), 1-8.

Sun, D., Gu, Q., Wen, H., Xu, J., Zhang, Y., Shi, S., Xue, M., & Zhou, X. (2023). Assessment of landslide susceptibility along mountain highways based on different machine learning algorithms and mapping units by hybrid factors screening and sample optimization. *Gondwana Research, 123*, 89–106. https://doi.org/10.1016/j.gr.2022.07.013

Sur, U., Singh, P., & Meena, SR. (2020). *Landslide susceptibility assessment in a lesser Himalayan road corridor (India) applying fuzzy AHP technique and earth-observation data*. Geomatics, Natural Hazards and Risk, 11(1), 2176–2209. https://doi.org/10.1080/19475705.2020.1836038

Upreti, BN., & Dhital, MR. (1996). *Landslide studies and management in Nepal* (Technical Publication). International Centre for Integrated Mountain Development. https://doi.org/10.53055/ICIMOD.240

Highland, L. (2004). *Landslide types and processes* (USGS Fact Sheet 2004-3072). U.S. Geological Survey. https://doi.org/10.3133/fs20043072

Varnes, DJ. (1978). Slope movement types and processes. In R. L. Schuster & R. J. Krizek (Eds.), *Landslides: Analysis and control* (Transportation Research Board Special Report No. 176, pp. 11–33). National Research Council.

Varnes, DJ., International Association of Engineering Geology Commission on Landslides and Other Mass Movements on Slopes. (1984). *Landslide hazard zonation: A review of principles and practice* (Natural Hazards, No. 3). UNESCO Press.

Yousefi, S., Jaafari, A., Valjarević, A., Gomez, C., Keesstra, S. (2022) Vulnerability assessment of road networks to landslide hazards in a dry-mountainous region. Environ Earth Sci 81(22):521. https://doi.org/10.1007/s12665-022-10650-z

Zhou, M., Yuan, M., Yang, G., Mei, G. (2024) Risk analysis of road networks under the influence of landslides by considering landslide susceptibility and road vulnerability: A case study. Nat Hazards Res 4(3):387–400. https://doi.org/10.1016/j.nhres.2023.09.013

Annexure-I:

Pairwise comparison matrix, consistency ratio and weights of the sub-criteria of the data layers

Slope Aspect

Slope	0° - 15°	15° - 25°	25° - 35°	35° - 45°	45° - 90°	Weights
0° - 15°	1	1/3	1/5	1/7	1/9	0.3575
15° - 25°	3	1	1/3	1/3	1/5	0.9733
25° - 35°	5	3	1	1/4	1/4	1.9000
35° - 45°	7	3	4	1	1/3	3.0667
45° - 90°	9	5	4	3	1	4.4000
Consistency Ratio: 0.04						

Normalized pairwise comparison matrix

Slope	0° - 15°	15° - 25°	25° - 35°	35° - 45°	45° - 90°	Weights
0° - 15°	0.040	0.027	0.021	0.031	0.059	0.0356

15° - 25°	0.120	0.081	0.035	0.037	0.106	0.0756
25° - 35°	0.200	0.243	0.105	0.055	0.132	0.1470
35° - 45°	0.280	0.243	0.420	0.219	0.176	0.2676
45° - 90°	0.360	0.405	0.420	0.658	0.528	0.4742
Sum	1	1	1	1	1	1

Aspect

Class	North	North-East	East	South East	South	South West	West	North West	Flat	Weights
North	1	1/2	1/3	1/5	1/7	1/5	1/2	1	8	0.052
North-East	2	1	1/2	1/2	1/3	1/2	1	1	8	0.085
East	3	2	1	1	1/2	1	1	2	8	0.135
South East	5	2	1	1	1	1	1	2	9	0.155
South	7	3	2	1	1	1	1	3	9	0.195
South West	5	2	1	1	1	1	1	3	9	0.162
West	2	1	1	1	1	1	1	2	8	0.132
North West	1	1	1/2	1/2	1/3	1/3	1/2	1	8	0.070
Flat	1/8	1/8	1/8	1/9	1/9	1/9	1/8	1/8	1	0.014
Consistency Ratio: 0.04										

Consistency calculation

slope	1	2	3	4	5	Sum	S/W
1	0.0356	0.0252	0.0294	0.0382286	0.052689	0.1811	5.087569
2	0.1068	0.0756	0.049	0.0446	0.09484	0.3708	4.905291
3	0.178	0.2268	0.147	0.0669	0.11855	0.7373	5.015306
4	0.2492	0.2268	0.588	0.2676	0.158067	1.4897	5.566766
5	0.3204	0.378	0.588	0.8028	0.4742	2.5634	5.405736

Curvature

Class	Negative	Zero	Positive	Weights
Negative	1	1	1/3	0.250
Zero	1	1	1	0.347
Positive	3	1	1	0.403
Consistency Ratio: 0.03				

Distance to Drainage

Class	0 – 850	850-1700	1700-2550	2550-3400	3400-4250	> 4250	Weights
	1	2	3	4	5	7	0.387
850-1700	1/2	1	2	3	4	5	0.249
1700-2550	1/3	1/2	1	2	3	4	0.160
2550-3400	1/4	1/3	1/2	1	2	2	0.094
3400-4250	1/5	1/4	1/3	1/2	1	2	0.066
> 4250	1/7	1/5	1/4	1/2	1/2	1	0.044
Consistency Ratio: 0.05							

Distance to Road

Type	0 – 850	850-1700	1700-2550	2550-3400	3400-4250	> 4250	Weights
0 – 850	1	2	3	4	5	6	0.379
850-1700	1/2	1	2	3	4	5	0.249

1700-2550	1/3	1/2	1	2	3	4	0.160
2550-3400	1/4	1/3	1/2	1	2	3	0.102
3400-4250	1/5	1/4	1/3	1/2	1	2	0.065
> 4250	1/6	1/5	1/4	1/3	1/2	1	0.043
Consistency Ratio: 0.01							

Rainfall

Type	>6.5	6.5-7.5	7.5-8.5	8.5-9.5	>9.5	Weights
<6.5	1	1/2	1/3	1/4	1/5	0.062
6.5-7.5	2	1	1/2	1/3	1/4	0.099
7.5-8.5	3	2	1	1/2	1/3	0.161
8.5-9.5	4	3	2	1	1/2	0.262
>9.5	5	4	3	2	1	0.416
Consistency Ratio: 0.03						

Drainage Density

Class	0-0.150	0.150-0.300	0.300 - 0.450	0.450 – 0.600	>0.600	Weights
0 - 0.150	1	1/2	1/3	1/4	1/5	0.062
0.150-0.300	2	1	1/2	1/3	1/4	0.099
0.300-0.450	3	2	1	1/2	1/3	0.161
0.450-0.600	4	3	2	1	1/2	0.262
>0.600	5	4	3	2	1	0.416
Consistency Ratio: 0.01						

LULC

Class	Build up Area	Agriculture land	Fores t	Shrub s	Gras s	Flooded vegetation	Bare land	Sno w	Water	Weights
Build up Area	1	1/2	1/8	1/4	1/4	1/2	1/9	3	9	0.058
Agriculture land	2	1	1/4	2	1/2	1	1/4	2	9	0.089
Forest	8	4	1	2	2	4	1	2	9	0.221
Shrubs	4	1/2	1/2	1	1	1/2	1/4	2	9	0.090
Grass	4	2	1/2	1	1	1/2	1/4	2	9	0.102
Flooded vegetation	2	1	1/4	2	2	1	1/4	2	9	0.103
Bare land	9	4	1	4	4	4	1	3	9	0.267
Snow	1/3	1/2	1/2	1/2	1/2	1/2	1/3	1	4	0.056
Water	1/9	1/9	1/9	1/9	1/9	1/9	1/9	1/4	1	0.014
Consistency Ration: 0.03										

Soil Type

Class	JMs	Ks	Pzl	Pzu	Ti	Trms	Pc	others	Weights
JMs	1	1/2	1/3	1/5	1/7	1/5	1/2	1	0.044291
Ks	2	1	1/2	1/2	1/3	1/2	1	1	0.082616
Pzl	3	2	1	1	1/2	1	1	2	0.138643
Pzu	5	2	1	1	1	1	1	2	0.16003
Ti	7	3	2	1	1	1	1	3	0.205024
Trms	5	2	1	1	1	1	1	3	0.168363
Pc	2	1	1	1	1	1	1	2	0.135607
others	1	1	1/2	1/2	1/3	1/3	1/2	1	0.065427

Consistency Ration: 1.14

Pairwise comparison matrix, factor weights and consistency ration of the data layers

SN	Factor	1	2	3	4	5	6	7	8	10	11	Weights
1	Aspect	1	1/2	2	2	1	2/3	1	1	2/3	1	0.085
2	Geology	2	1	3	2	2	1	2	2	1	3	0.145
3	Curvature	1/2	1/3	1	1/2	1/2	1/3	1/2	1/2	1/3	1	0.043
4	DR	1/2	1/2	2	1	1	2/3	1	1	1/2	1	0.074
5	DD	1	1/2	2	1	1	2/3	1	1/2	2	1	0.087
6	Slope	2	1	5	3	3	1	2	2	1	3	0.129
7	Landuse	1	1/2	2	1	1	2/3	1	1	2/3	2	0.084
8	Rainfall	1	1/2	2	1	2	2/3	1	1	2/3	2	0.09
9	Soil	2	1	3	2	1 1/2	1	1 1/2	1 1/2	1	1 1/2	0.115
10	Drainage density	1	1/3	1	1	1	1/3	1/2	1/2	2/3	1	0.053

Consistency Ratio: 0.06

$$\lambda_{max} = \frac{S/W}{n} = 5.1961$$

Consistency index (CI) $= \frac{\lambda_{max}-n}{n-1} = \frac{5.1961-5}{5-1} = 0.0490$

Consistency Ration (CR) = $\frac{0.0490}{1.12} = 0.0437$